

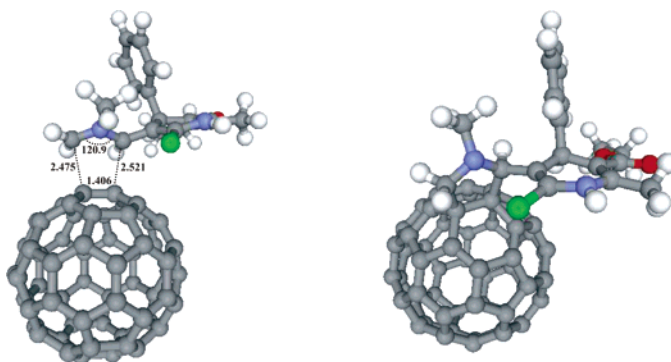
Theoretical Study of the Highly Diastereoselective 1,3-Dipolar Cycloaddition of 1,4-Dihydropyridine-Containing Azomethine Ylides to [60]Fullerene (Prato's Reaction)

Amaury Alvarez,<sup>†,‡</sup> Estael Ochoa,<sup>†</sup> Yamila Verdecia,<sup>†</sup> Margarita Suárez,<sup>\*,†</sup> Miquel Solá,<sup>\*,§</sup> and Nazario Martín<sup>\*,||</sup>

Laboratorio de Síntesis Orgánica, Facultad de Química, Universidad de La Habana, 10400 Ciudad Habana, Cuba, Instituto Cubano de Investigaciones de los Derivados de la Caña de Azúcar, P.O. Box 4026, Ciudad Habana, Cuba, Institut de Química Computacional and Departament de Química, Universitat de Girona, 17071 Girona, Catalonia, Spain, and Departamento de Química Orgánica, Facultad de Química, Universidad Complutense, 28040 Madrid, Spain

msuarez@fq.uh.cu; nazmar@quim.ucm.es; miquel.sola@udg.es

Received November 25, 2004



The 1,3-dipolar cycloaddition of azomethine ylides bearing the biologically active 1,4-dihydropyridine ring to C<sub>60</sub> was investigated by means of quantum mechanical calculations at the semiempirical AM1 and DFT (B3LYP/6-31G\*) methods. The presence of two chiral centers and one chiral axis in the resulting fulleropyrrolidines leads to four possible [6,6] cycloaddition products. Formation of atropisomers has also been considered. The transition-state structures were computed for the four different cycloaddition pathways to find out the lowest activation energy stereoisomer. In all cases, a frequency analysis and an IRC calculation were carried out to fully characterize the located transition-state structures. AM1 results and single-point energy calculations at the B3LYP/6-31G\*\*/AM1 level for the four transition-state structures yield activation energies values below 5 kcal/mol.

## Introduction

The surge of interest in fullerenes chemistry has extensively been focused on the functionalization of C<sub>60</sub>, the most abundant and representative of fullerenes. The chemical derivatization of fullerenes still represents an important challenge in current chemical research, and among the wide variety of organofullerenes synthesized by simple and accessible synthetic routes, the family of fulleropyrrolidines has played a prominent role provided

that they retain the basic fullerene properties and are commonly soluble in organic solvents.<sup>1</sup>

The electron-deficient character of C<sub>60</sub> stems from its low-lying LUMO, and therefore, all embedded olefins ([6-6]-ring junctions) in the fullerene cage behave as strong electrophiles, which prompted the development of numerous efficient cycloadditions.<sup>2,3</sup> Among them, one of the most used and successful reactions has been the 1,3

(1) Tagmatarchis, N.; Prato, M. *Synlett* **2003**, 768.

(2) (a) Hirsch, A.; Brettreich, M.; Wuld, F. *Fullerenes: Chemistry and Reactions*; John Wiley and Sons Ltd.: New York, 2004. (b) Diederich, E.; Thilgen, C. *Science* **1996**, 271, 317. (c) Hirsch, A. *Fullerenes and Related Structures*; Springer: Berlin, 1999. (d) *Fullerenes and Related Structures*; Hirsch, A., Ed. *Top. Curr. Chem.* **1999**, 199, 1.

<sup>†</sup> Universidad de La Habana.

<sup>‡</sup> Instituto Cubano de Investigaciones de los Derivados de la Caña de Azúcar.

<sup>§</sup> Universitat de Girona.

<sup>||</sup> Universidad Complutense.

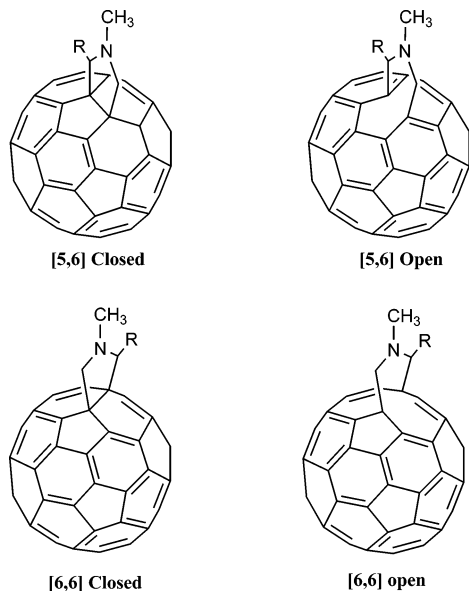


**FIGURE 1.** Four possible regioisomers from a 1,3-dipolar cycloaddition of azomethine ylides to  $C_{60}$ . Only the [6,6] closed regioisomer is formed.

dipolar cycloaddition (1,3-DC) of azomethine ylides to  $C_{60}$ .<sup>4</sup> Although this reaction has been extensively employed for the functionalization of  $C_{60}$ , there are few theoretical reports on its mechanism,<sup>5</sup> especially when the 1,3 dipole is endowed with a large organic addend and the reaction can lead to more than one product.

Theoretically, the 1,3-dipolar cycloaddition reaction could take place at both [5,6] and [6,6] junctions of the fullerene surface leading to the formation of four regioisomers (Figure 1); however, previous studies showed that only the closed [6,6] product is formed.<sup>1,4-7</sup>

Recently, we have carried out the synthesis of novel fulleropyrrolidines bearing biologically active 1,4-dihydropyridines (1,4-DHP) (**3**) as potential channel modulators for the treatment of cardiovascular disorders.<sup>8,9</sup> The fullerene derivatives were synthesized by 1,3-dipolar cycloaddition of the in situ generated azomethine ylide (**2**) to  $C_{60}$  by heating in *o*-dichlorobenzene (*o*-DCB) the corresponding formyl-substituted 1,4-DHP (**1**)<sup>9</sup> with sarcosine (*N*-methylglycine) and [60]fullerene, following Prato's protocol<sup>4</sup> (see Scheme 1).

We also reported the calculated heats of formation for the four expected stereoisomers, considering only the two

stereogenic centers in compound **3** (see Scheme 1). Stereoisomer *RS* was found to be the most stable one.<sup>8</sup> To gain a better understanding of this complex cycloaddition process, in this work the reaction paths as well as the transition state structures affording different reaction products were analyzed by semiempirical (AM1) and ab initio methods (B3LYP/6-31G\*).

In this regard, Huisgen's pioneering works have provided a general description of the 1,3-DC reactions in which the 1,3-dipole, represented by a zwitterionic species, reacts with a dipolarophile molecule containing a multiple bond to form five-membered heterocyclic systems.<sup>10</sup> The minor effect of solvent polarity on the reaction rate, together with the high regioselectivity observed, provided support for a concerted reaction pathway.<sup>11</sup> For this reason, in the present work only the concerted mechanism has been analyzed.

## Method of Calculation

Full geometry optimizations without symmetry restrictions have been carried out using the AM1 semiempirical method<sup>12</sup> implemented in Gaussian 98.<sup>13</sup> All zero-gradient structures have been characterized by a vibrational analysis. For all transition-state structures, the intrinsic reaction coordinate (IRC)<sup>14</sup> was followed with the AM1 method to make sure that each transition state connects the expected reactants and products. For all the stationary points, single-point B3LYP/6-31G\*<sup>15</sup> energy calculations have been performed using the AM1-optimized geometry with help of the Gaussian 98 program. The transition-state structures were found using the QST3<sup>16</sup> method implemented in Gaussian 98; all the transition state structures have only one imaginary frequency which is interpreted as negative vibrational mode (physically the approach of the reaction centers).<sup>17</sup>

(9) (a) Illescas, B. M.; Martínez-Grau, M. A.; Torres, M. L.; Fernández-Gadea, J.; Martín, N. *Tetrahedron Lett.* **2002**, *43*, 4133. (b) Illescas, B. M.; Martínez-Alvarez, R.; Fernández-Gadea, J.; Martín, N. *Tetrahedron* **2003**, *59*, 6569.

(10) (a) Huisgen, R. *Angew. Chem., Int. Ed. Engl.* **1963**, *2*, 565. (b) Huisgen, R. *Angew. Chem., Int. Ed. Engl.* **1963**, *2*, 633.

(11) (a) L'Abbé, G. *Chem. Rev.* **1969**, *69*, 345. (b) Houk, K. N.; González, J.; Li, Y. *Acc. Chem. Res.* **1995**, *28*, 81. (c) Gothelf, K. V.; Jorgensen, K. A. *Chem. Rev.* **1998**, *98*, 863.

(12) Dewar, M. J. S.; Zoebisch, E. G.; Healy, E. F.; Stewart, J. J. P. *J. Am. Chem. Soc.* **1985**, *107*, 3902.

(13) Frisch, M. J.; Trucks, G. W.; Schlegel, H. B.; Scuseria, G. E.; Robb, M. A.; Cheeseman, J. R.; Zakrzewski, V. G.; Montgomery, J. A., Jr.; Stratmann, R. E.; Burant, J. C.; Dapprich, S.; Millam, J. M.; Daniels, A. D.; Kudin, K. N.; Strain, M. C.; Farkas, O.; Tomasi, J.; Barone, V.; Cossi, M.; Cammi, R.; Mennucci, B.; Pomelli, C.; Adamo, C.; Clifford, S.; Ochterski, J.; Petersson, G. A.; Ayala, P. Y.; Cui, Q.; Morokuma, K.; Malick, D. K.; Rabuck, A. D.; Raghavachari, K.; Foresman, J. B.; Cioslowski, J.; Ortiz, J. V.; Stefanov, B. B.; Liu, G.; Liashenko, A.; Piskorz, P.; Komaromi, I.; Gomperts, R.; Martin, R. L.; Fox, D. J.; Keith, T.; Al-Laham, M. A.; Peng, C. Y.; Nanayakkara, A.; Gonzalez, C.; Challacombe, M.; Gill, P. M. W.; Johnson, B.; Chen, W.; Wong, M. W.; Andres, J. L.; Gonzalez, C.; Head-Gordon, M.; Replogle, E. S.; Pople, J. A. *Gaussian 98, Revision A.3*; Gaussian, Inc.: Pittsburgh, PA, 1998.

(14) (a) Gonzales, C.; Schlegel, H. B. *J. Chem. Phys.* **1989**, *90*, 2154. (b) Gonzales, C.; Schlegel, H. B. *J. Phys. Chem.* **1990**, *94*, 5523.

(15) (a) Binkley, J. S.; Pople, J. A.; Hehre, W. J. *J. Am. Chem. Soc.* **1980**, *102*, 939. (b) Gordon, M. S.; Binkley, J. S.; Pople, J. A.; Pietro, W. J.; Hehre, W. J. *J. Am. Chem. Soc.* **1982**, *104*, 2797. (c) Pietro, W. J.; Francl, M. M.; Hehre, W. J.; Defrees, D. J.; Pople, J. A.; Binkley, J. S. *J. Am. Chem. Soc.* **1982**, *104*, 5039. (d) Becke, A. D. *J. Chem. Phys.* **1993**, *98*, 5648. (e) Lee, C.; Yang, W.; Parr, R. G. *Phys. Rev. B* **1988**, *37*, 785. (f) Stephens, P. J.; Devlin, F. J.; Chabalowski, C. F.; Frisch, M. J. *J. Phys. Chem.* **1994**, *98*, 11623.

(16) Peng, C.; Schlegel, H. B. *Israel J. Chem.* **1994**, *33*, 449.

(17) Young, D. C. *Computational Chemistry: A Practical Guide for Applying Techniques to Real-World Problems*; John Wiley & Sons, Inc.: New York, 2001; ISBN 0-471-22065-5 (electronic).

(3) Guldi, D. M.; Martín, N., Eds. *Fullerenes: From Synthesis to Optoelectronic Properties*; Kluwer Academic Publishers: Dordrecht, 2002.

(4) (a) Maggini, M.; Scorrano, G.; Prato, M. *J. Am. Chem. Soc.* **1993**, *115*, 9798. (b) Novello, F.; Prato, M.; Ros, T. D.; Amici, M. D.; Bianco, A.; Toniolo, C.; Maggini, M. *J. Chem. Soc., Chem. Commun.* **1996**, 903. (c) Prato, M.; Maggini, M. *Acc. Chem. Res.* **1998**, *31*, 519.

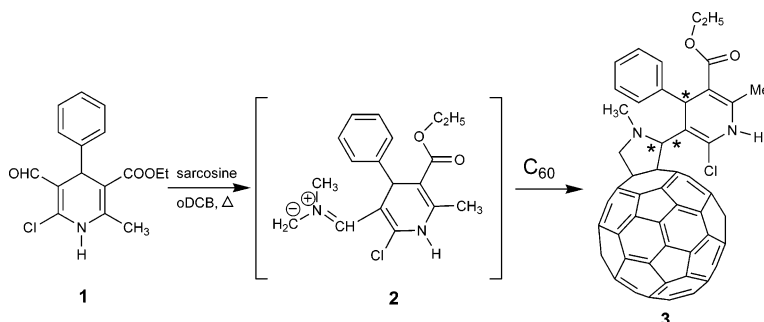
(5) Cases, M.; Duran, M.; Mestres, J.; Martín, N.; Solà, M. *J. Org. Chem.* **2001**, 433 and references therein.

(6) (a) Turker, L. *THEOCHEM* **2002**, *588*, 165. (b) Cases, M.; Duran, M.; Mestres, J.; Martín, N.; Solà, M. In *Fullerenes for the New Millennium*; Kamat, P. V., Kadish, K. M., Guldi, D. M., Eds.; The Electrochemical Society, Inc.: Pennington, 2001; Vol. 11, p 244.

(7) (a) Helaja, J.; Tauber, A. Y.; Abel, Y.; Tkachenko, N. V.; Lemmetyinen, H.; Kilpeläinen, I.; Hynninen, P. H. *J. Chem. Soc., Perkin Trans. 1* **1999**, 2403. (b) Sandall, J. P. B.; Fowler, P. W.; Taylor, R. *J. Chem. Soc., Perkin Trans. 2* **2002**, 1718.

(8) Suárez, M.; Verdecia, Y.; Illescas, B.; Martínez-Alvarez, R.; Alvarez, A.; Ochoa, E.; Seoane, C.; Kayali, N.; Martín, N. *Tetrahedron* **2003**, *59*, 9179.

## SCHEME 1. 1,3-Dipolar Cycloaddition of Azomethine Ylide (2) to Fullerene



## Results and Discussion

The starting geometries of the reactants were optimized by means of molecular mechanics with the aid of the Hyperchem<sup>18</sup> program. The structure of the C<sub>60</sub> moiety was obtained from the Hyperchem database.<sup>18</sup> Figure 2 shows the minimum energy conformation of the azomethine ylide (2). The presence of one stereogenic center (C9) and two prochiral faces (*re* and *si*) could lead to, at least, four different stereoisomers.

The atoms C5, N1, and C2 in the intermediate 2 (see Figure 2) form a prochiral plane with two prochiral faces. Thus, the configuration of the chiral center at C2 in the final product 3 (see Scheme 1) will depend on the reacting prochiral face. Also, the C2–C8 bond could be a chiral axis if the rotation around this bond is restricted in 3. It is not obvious whether the rotation across the C2–C8 bond connecting the pyrrolidine and the 1,4-dihydropyridine rings is restricted by the presence of the chlorine atom on C7 and the phenyl substituent on C9, which may interact with the fullerene cage. If this barrier is high enough, then the bond is a chiral axis (denoted by *S<sub>a</sub>* or *R<sub>a</sub>*) and additional stereoisomers could exist, leading at least to eight different stereoisomers.

To establish whether the C2–C8 bond is a chiral axis or not, we have calculated the rotational barrier around this bond for the *R* and *S* configurations of the stereogenic center at C2. Figure 3 shows the conformational study carried out by using B3LYP/6-31G\*\*/AM1 calculations.

The predicted energy barrier to transform A<sub>1</sub> (*RSaS* configuration) into C<sub>1</sub> (*RRaS* configuration) across B is 28.9 kcal/mol, and the energy necessary to transform C<sub>1</sub> (*RRaS* configuration) into A<sub>1</sub> (*RSaS* configuration) across D is 40.4 kcal/mol for the *R* configuration at C2. For the *S* configuration at C2 the predicted barrier is 23.8 kcal/mol for the transformation of A<sub>2</sub> (*SSaS* configuration) to C<sub>2</sub> (*SRaS* configuration) across B, and from C<sub>2</sub> to A<sub>2</sub> this

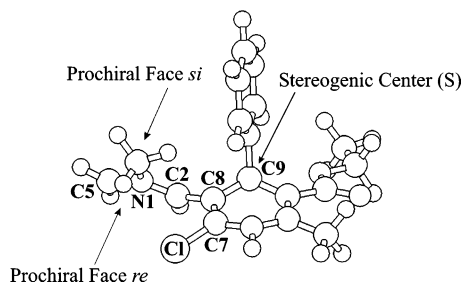


**FIGURE 2.** Minimum energy conformation (AM1) of the azomethine ylide (2) showing symmetry elements and the numbering scheme.

barrier is 20.1 kcal/mol. This energy barrier values fall into the range that corresponds to atropoisomers.<sup>19</sup> It is important to mention that studies about atropoisomerism involving fulleropyrrolidines have not been previously reported.

The results show that the C2–C8 bond is a chiral axis and **A** and **C** represent the different configurations of the chiral axis. Thus, **A** corresponds to the *S<sub>a</sub>* and **C** to the *R<sub>a</sub>* axis configuration of the axis. Therefore, three chiral elements are present in the molecule, and accordingly, eight stereoisomers should exist, four of them as enantiomeric pairs. Table 1 shows the symmetry elements involved and the heats of formation corresponding to each pair of enantiomers. The classification of the chiral axis was made following the Cahn–Ingold–Prelog rules (CIP).<sup>20</sup> Figure 4 shows the line drawings showing the configuration of the stereogenic centers as well as the relationship existing between the different stereoisomers.

Figure 5 shows the minimum energy conformation found for four of the eight stereoisomers; only the *S<sub>a</sub>* configuration is shown for clarity.

Once the relationship existing between the possible products was established, it was important to predict which of them would be most likely formed. To accomplish this task, the mechanism of the 1,3-DC was studied. Initially, to test the reliability of our approach, we calculated the energy barriers for a smaller and simpler model system (ethylene and the azomethine ylide leading to a pyrrolidine ring) at different theory levels,

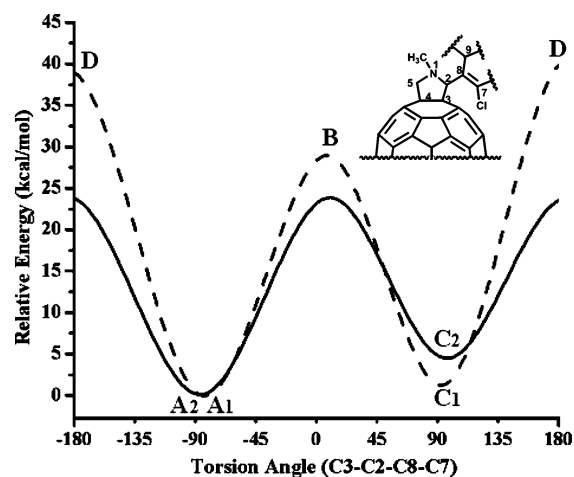


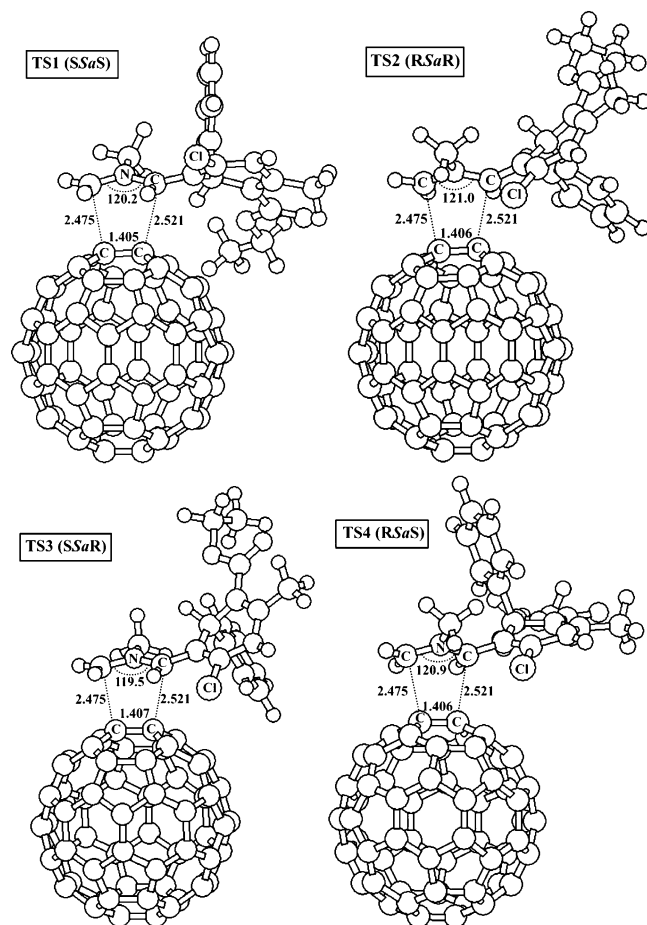
**FIGURE 3.** Rotational energy profile across the C3–C2–C8–C7 dihedral angle at the B3LYP/6-31G\*\*/AM1 level, for the *S* (solid line) and for the *R* (dashed line) configurations at C2 in compound 3.



**TABLE 2.** Energy Barriers and Reaction Energies for the 1,3-DC of Azomethine Ylide to Ethylene at Different Theory Levels (Energies Are Given in kcal/mol)

method	$\Delta E^\ddagger$	$\Delta E_r$	method	$\Delta E^\ddagger$	$\Delta E_r$
AM1 <sup>a</sup>	5.7	-70.3	B3LYP/6-31G*	1.2	-68.6
HF/6-31G**//AM1	11.7	-92.9	B3LYP/6-311++G**	3.9	-59.2
HF/6-31G*	10.8	-95.9	QCISD/6-31G*	3.1	-77.8
B3LYP/6-31G**//AM1	1.3	-64.6	CCSD(T)/6-311++G**//QCISD/6-31G*	-0.1	-71.8

<sup>a</sup> For the AM1 method, the energies are enthalpies at 298 K.

**FIGURE 6.** Transition-state structures leading to the four different stereoisomers.

show that each transition state has only one imaginary vibrational frequency<sup>17</sup> (see Table 3).

Figure 7 shows the IRC<sup>14</sup> study in mass-weighted internal coordinates that was carried out using the AM1 semiempirical method. The force constants were calculated at the first point. The geometry was optimized at each point along the fifteen points in each direction of the reaction coordinate. The step size was 0.1 amu<sup>1/2</sup> bohr. The results clearly show that the transition-state structures found connect the expected reactants and products.

As expected, the found geometries for the different transition states were very similar since the reaction centers are the same for all cases. The energy differences observed between them can be accounted for by steric and/or electronic repulsions between the chlorine atom on C7 and the phenyl substituent on C9 of the 1,4-dihydropyridine ring with the fullerene cage, this being also the reason for the hindered rotation (Figure 8). The hydrogen atom at the C2 (H2) may interact in some cases

with the chlorine atom, depending on the reacting prochiral face, resulting in a lowering of the transition-state energy. In addition, the favorable release of energy resulting from the saturation of one fullerene double bond (about 8 kcal/mol for each carbon atom)<sup>3</sup> was also applied in all cases. Figure 8 shows the expanded transition-state structure of the most stable TS1 (SSaS) transition state and the numbering scheme used. Table 3 collects some of the most significant geometrical and electronic parameters for the four studied transition states.

The close bond distances and angles in the transition-state structures (see Figure 6 and Table 3) can be accounted for by the similarity between these structures. The difference in energy is due to the different spatial arrangement of the atoms in the four transition states (as shown in Figure 7).

The dihedral angle C8-C2-N1-C6 in the transition-state structures TS1 (SSaS) and TS3 (SSaR) has a positive value, which implies that the methyl group on N1 is on the opposite side of the chlorine atom. The fact that the methyl group is on the same side of the molecule (and opposite to the 1,4-DHP ring) in both TS1 and TS3 is related to the configuration of the stereogenic center at C7 (see Figure 6) or, in a more appropriate way, of which prochiral face of the molecule **2** reacts.

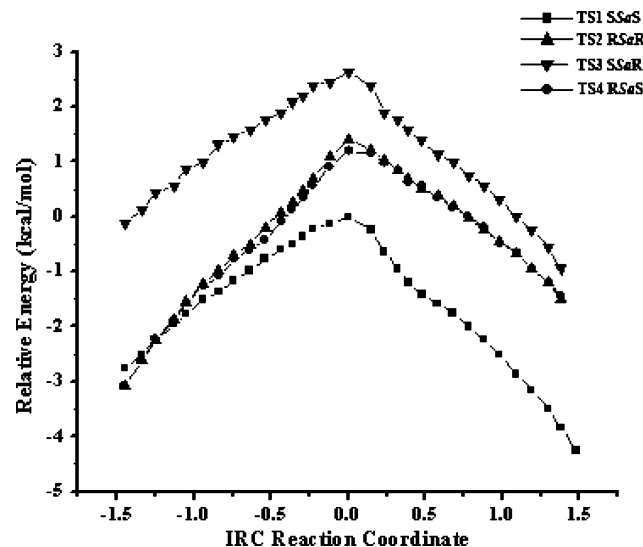
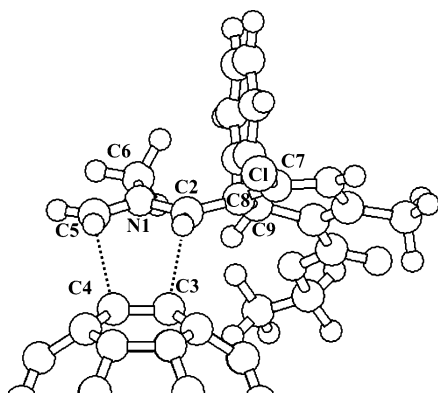
The distance between the hydrogen atom in C2 (H2) and the chlorine atom seems to be the major reason for the energetic difference between the *S* and *R* configurations of the C2 stereogenic center (Figure 2). When the *si* prochiral face of the molecule reacts, the distance between the H2 and the chlorine atom is shorter: 2.52 Å for TS3 and 2.60 Å for TS1. However, the configuration of the second stereogenic center is important since the *R* configuration of this center brings the phenyl substituent near the fullerene cage and this raises the energy of the TS. The fact that the TS1 (SSaS) has the lower activation energy can be accounted for by the proximity of H2 and Cl atoms and the favorable electrostatic interaction between them. When we analyze the TS3 (SSaR) again, the same interaction is also present. However, the configuration of the second stereogenic center (*R* in this case) brings the phenyl substituent near to the fullerene cage and, to avoid this interaction, the structure is more strained, resulting in the most energetic of the four

(22) (a) Cativiela, C.; Díaz-de-Villegas, M. D.; García, J. I.; Jiménez, A. I. *Tetrahedron* **1997**, *55*, 4479. (b) Dewar, M. J. S.; Hwang, J. C.; Kuhn, D. R. *J. Am. Chem. Soc.* **1991**, *113*, 735. (c) Ponc, R.; Yuzhakov, G.; Haas, Y.; Samuni, U. *J. Org. Chem.* **1997**, *62*, 2757. (d) Houk, K. N. *Angew. Chem., Int. Ed. Engl.* **1992**, *31*, 682. (e) Borden, W. T.; Loncharich, R. J.; Houk, K. N. *Annu. Rev. Phys. Chem.* **1988**, *39*, 213. (f) Dewar, M. J. S.; Olivella, S.; Stewart, J. J. P. *J. Am. Chem. Soc.* **1986**, *108*, 5771. (g) Solà, M.; Mestres, J.; Martí, J.; Duran, M. *Chem. Phys. Lett.* **1994**, *231*, 325. (h) Mestres, J.; Duran, M.; Solà, M. *J. Phys. Chem.* **1996**, *100*, 7449. (i) Solà, M.; Duran, M.; Mestres, J. *J. Am. Chem. Soc.* **1996**, *118*, 8920. (j) Mestres, J.; Solà, M. *J. Org. Chem.* **1998**, *63*, 7556.

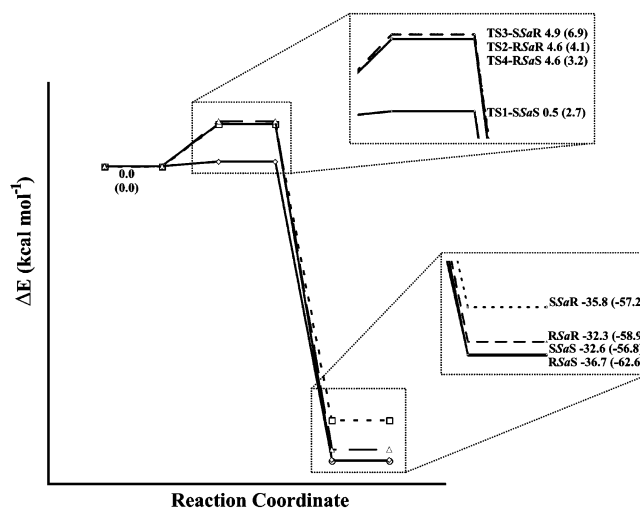
**TABLE 3.** Main Structural and Energetic Characteristics for the Four Calculated Transition States<sup>a</sup>

	C8–C2–N1–C6	H2–Cl	frequency	$\mu$	$\Delta E^\ddagger$	$\Delta E_r$	$\Delta H^\ddagger$ (AM1)	$\Delta H_r$ (AM1)
TS1-SSaS	8.9	2.604	145.5i	6.6	0.5	-32.6	2.7	-56.8
TS2-RSaR	-16.6	4.121	129.9i	6.6	4.6	-32.3	4.1	-58.9
TS3-SSaR	25.1	2.518	136.2i	6.3	4.9	-35.8	6.9	-57.2
TS4-RSaS	-13.0	4.136	122.0i	7.1	4.6	-36.7	3.2	-62.6

<sup>a</sup> Frequency in  $\text{cm}^{-1}$ . Distances in Å and dihedral angles in deg. Dipolar moments in debyes and the energies in kcal/mol. The  $\Delta E^\ddagger$  values are the difference between the energies (B3LYP/6-31-G\*\*//AM1) of the transition-state structures and the reactants, while the  $\Delta E_r$  values are the difference between the energies (B3LYP/6-31-G\*\*//AM1) of the reactants and the products.  $\Delta H^\ddagger$  and  $\Delta H_r$  are the differences in AM1 enthalpies of formation of transition state and reactants and of products and reactants, respectively. Only the structures corresponding to the *Sa* configuration were analyzed; each structure has an enantiomeric pair (not shown).

**FIGURE 7.** IRC for the four different transition-state structures (AM1). The TS1 (SSaS) transition state was chosen as the zero energy point.**FIGURE 8.** Numbering scheme used for the transition-state structures (TS1-SSaS is shown).

studied transition states. In the TS4 (RSaS) and TS2 (RSaR) transition states, both have the same activation energy and it is not clear which will be the most favored path (see Table 3). The *R* configuration of the second stereogenic center can interact again with the fullerene cage in TS2, making the TS4 somehow more favored. The values of the reaction energies (between -32.3 and -36.7 kcal/mol) show that the retrocycloaddition is not likely to occur, and therefore, a thermodynamic control of the reaction can be ruled out. The low activation energies and the high barrier for the retrocycloaddition point to a kinetically controlled reaction in which one of the prod-

**FIGURE 9.** Energy profile for the reaction of the azomethine ylide to  $\text{C}_{60}$  calculated by the B3LYP/6-31G\*\*//AM1(AM1) method. AM1 energies are enthalpies at 298 K.

ucts will be formed in a very high ratio in comparison to the other products. This is in agreement with the experimental spectroscopic data that show the formation of stereoisomers in a 95/5 ratio.<sup>8</sup> The most abundant stereoisomer should have a SSaS configuration. It is important to note that the AM1 results follow the same trend found at the higher level ab initio calculations. This fact gives support to the semiempirical methods as a useful tool for treating large systems with reasonable good results.

In summary, Figure 9 depicts the reaction energy profile calculated for the four cycloadditions analyzed at the B3LYP/6-31G\*\*//AM1 level. As one may expect from the fact that we have studied a thermally allowed cycloaddition,<sup>23</sup> the analysis of the energy profile shows that these cycloaddition reactions are quite exothermic and have low activation energies, in agreement with experimental results.<sup>4</sup>

## Conclusions

The activation energy for the four calculated transition-state structures is around 4 kcal/mol and the difference between them is very low, which can be accounted for by the similarity of these structures. In all cases, frequency analysis and IRC were performed to fully characterize the four transition states for the 1,3-DC

(23) Lowry, T. H.; Richardson, K. S. *Mechanism and Theory in Organic Chemistry*, 3rd ed.; Benjamin-Cummings Publishing Co.: Menlo Park, CA, 1987.

reactions. The energetic differences found for the transition states are steric and/or electronic hindrance caused by the size of the organic addend attached to the 1,3-dipole. However, the formation of the *SSaS* stereoisomer is favored over the other products, which seems to be a kinetically controlled reaction. Formation of other stereoisomers is less likely to occur and the *RSaS* stereoisomer is slightly more favorable because of steric factors. These findings are in agreement with the spectroscopic data that show for the modeled reaction the presence of a product constituted by two stereoisomers in a 95/5 ratio.

**Acknowledgment.** This work has been supported by the Alma Mater Project of Universidad de La Habana and MCYT of Spain (Project Nos. BQU2002-00855 and BQU2002-0412-C02-02). M. Suárez is grateful for SAB2003-0161 from Secretaria de Estado de

Universidad e Investigación del Ministerio de Educación y Ciencia de España. M. Solá is indebted to the DURSI of the Generalitat de Catalunya for financial support through the Distinguished University Research Promotion, 2001.

**Supporting Information Available:** Computational details, total energies, and relative energies of the reaction between the azomethine ylide and the ethylene and from the reaction between fullerene and the azomethine ylide bearing the 1,4-DHP moiety. Geometries of reactants, products, and transition state corresponding to the reaction between the azomethine ylide and the ethylene (XYZ) and between the azomethine ylide and fullerene (Z matrix). Molecular geometries (AM1) corresponding to the eight possible stereoisomers. This material is available free of charge via the Internet at <http://pubs.acs.org>.

JO0479009